7.4   **THE ROLE OF SATELLITE-DERIVED CLOUD CLIMATOLOGIES IN DEEP-SPACE TO GROUND LASER COMMUNICATIONS**

Gary S. Wojcik,* Heather L. Szymczak, Randall J. Alliss, Michael L. Mason

Northrop Grumman Information Technology TASC, Chantilly, Virginia

1. INTRODUCTION

NASA's Jet Propulsion Laboratory is investigating strategies to support high availability laser communications for future missions to Mars and for communicating with future stations on the Moon. Such projects will generate an ever increasing amount of data that must be transferred to ground locations. As an alternative to the current use of radio communications, deep-space to ground laser communications will provide a higher bandwidth to transfer these data with smaller power mass and power consumption subsystems. Optical communications may be interrupted by cloud cover. Therefore, a mitigation strategy ensuring a high likelihood of a cloud-free line of sight (CFLOS) between a ground station and a spacecraft or probe is needed to maximize the transfer of data. One strategy to address this problem is the use of *ground station diversity* in which several stations are *available* to receive communications should one or more sites be cloud covered or unreachable. For our purposes, we define *availability* to be the fraction of time that at least one station in the network has CFLOS and has a communication link with a probe. In this paper, we discuss our work for JPL in which we generate networks of different sizes with optimal availabilities.

The availability of a communication link between a probe and a ground station network depends on many factors including cloud cover, the number and location of sites in the network and the orbit of the spacecraft, which determines its elevation angle and the path length of transmission through the atmosphere. Typical meteorological patterns cause the cloud cover state within 100 to 200 kilometers to be correlated. Consequently, stations within the network should be placed far enough apart to diminish correlations. Shaik et al. (1993) suggest that this distance be a minimum of 150 km based on cloud-system correlation coefficients between sites as developed from empirical information from the Air Force Geophysics Laboratory. This requirement may lead to the selection of a station that

---
Corresponding author address: Gary S.Wojcik, Northrop Grumman Information Technology TASC, 4801 Stonecroft Blvd., Chantilly, VA 20151. E-mail: gary.wojcik@ngc.com

has a lower CFLOS than sites not selected but is less correlated with other network sites. Stations also need to be close enough to each other to produce a continuous communication link with the probe as the probe's position with respect to the ground changes with time.

The strength of the optical signal reaching a ground station depends not only on cloud cover but also the amount of atmospheric turbulence in the line of sight, the amount of atmospheric scattering from the beam due to aerosols, in particular, and the brightness of the background sky. To help alleviate these issues, stations should be placed at higher altitudes where the atmosphere is thinner and where turbulence and aerosol loadings are reduced (Shaik et al. 1993, Piazzolla et al. 2004). As altitude increases, the percentage of available land decreases, restricting the number of possible locations for ground stations. In fact, over the latitude range of $\pm40°$, a range selected to be better able to track a spacecraft in the solar ecliptic, 3.5 % of the Earth's land mass is above 1 km and 1.2 % is above 2 km (Piazzolla et al. 2004). Also, the elevation angle of the probe with respect to ground stations should be greater than 20° to reduce the path length of transmission between the probe and ground stations (Piazzolla et al. 2004).

Previous studies have defined regions favorable for ground station locations and configurations of the ground station networks across the globe (Shaik et al. 1993, Piazzolla et al. 2004). Considering cloud cover, atmospheric transmission, technical characteristics of telescopes and optical systems, and a probe in Pluto orbit, Shaik et al. (1993) determined availabilities of networks in the linear dispersed optical subnet (LDOS) and clustered optical subnet (COS) configurations. The LDOS networks contain stations located approximately evenly spaced longitudinally across the globe. The COS networks consist of several clusters of three or more stations no more than a few hundred kilometers apart, with each cluster spaced evenly across the globe longitudinally. The COS configuration allows the probe to communicate with one of the stations in a cluster if one or more stations are down due to weather or other problems. Shaik et al. found that an LDOS with six stations could produce an 81 % weather availability

and full coverage for the network and a COS network of three groups of four stations gives full network coverage and an availability of 96 %. The final recommendation from Shaik et al. is to use an LDOS network with six to eight stations since this meets or exceeds the network goals with the fewest number of stations.

With cloud data from the International Satellite Cloud Climatology Project (ISCCP) and high resolution topography data, Piazzolla et al. (2004) isolated several favorable regions for potential ground stations. These regions, which had average annual cloud cover of less than 50 % and altitudes higher than 1 km, included the southwestern continental United States (CONUS), Hawaii, Chile, Peru, Ecuador, Spain, Canary Islands, southern Africa, Yemen, Israel, Iran, Pakistan, and a few locations in Australia.

While these two studies provided significant progress in addressing the challenge of selecting stations for an optical network, they also have limitations with respect to the cloud data analyzed. Both studies used cloud data with limited temporal, spectral, and/or spatial resolution. The ISCCP data used by both Shaik et al. (1993) and by Piazzolla et al. (2004) have a spatial resolution of 250 km and miss smaller features of the cloud environment. Because telescopes are essentially point locations, a higher spatial resolution of cloud data will be beneficial to selecting ground station locations.

The work reported here implements methodologies different than the two studies discussed above to determine optimal ground station networks. The networks that we generated were determined with an optimization scheme that can distinguish and rank site availability based on a multi-year cloud climatology for many locations around the globe and based on the movement and location of the probe. Previous studies by TASC for JPL have focused on limited domains in CONUS, Hawaii, and South America (Alliss et al. 2004, Link et al. 2005). Networks derived from these limited domains have their availabilities penalized for the times when the probe is below the horizon (i.e., no communication link). More recent work has focused on several regions around the globe (Wojcik et al. 2005). The current study is a continuation of the Wojcik et al. (2005) study. Cloud mask data from selected regions in CONUS, Hawaii, South America, Europe, northern and southern Africa, the Middle East, central and eastern Asia, and Australia are analyzed with the TASC Lasercom Network Optimization Tool (LNOT). LNOT is an in-house software that applies an optimization routine to cloud mask data and probe location to determine networks of stations with optimal availabilities. By expanding the domains of interest to include regions around the world, the probe is more frequently visible to at least one station in the network, increasing availabilities.

Cloud masks, two-dimensional projections of clouds on the surface that show the horizontal location of clouds as seen from a satellite, have been created with TASC's Cloud Mask Generator (CMG). CMG uses several threshold tests involving radiance-derived cloud identifications tools (i.e., fog product, albedo product) calculated from the Geostationary Operational Environmental Satellite (GOES) and European Organization for the Exploitation of Meteorological Satellites (EUMETSAT) Meteosat satellite data to determine the likelihood of cloud cover in a given satellite pixel.

The methodology that we employ, including descriptions of the satellite data, CMG, and LNOT are discussed in section 2. Section 3 contains a discussion of single site CFLOS for several sites of interest. The networks availabilities are also presented in section 3. The results are summarized and their implications discussed in section 4.

2. METHODOLOGY

2.1. Cloud Analysis

2.1.1. Satellite Data

The analysis period presented here extends from June 2003 through May 2004. Note that our database of satellite images for CONUS and Hawaii stretches from 1995 to present, while the database for the other regions and sites of interest (Table 1; Fig. 1) contains data from June 2003 to present. The data for regions in the western part of CONUS and Hawaii are from GOES-West, while those for South America and the eastern part of CONUS come from GOES-East. GOES-9 provided the data for the Australia and China regions. Data for regions in Europe and Africa are from Meteosat-7, while those for the Middle East and central Asia regions are from Meteosat-5. For the period of interest, satellite data for CONUS and Hawaii are at 15 min resolution while the resolution for the South America, Europe, and Africa regions is 30 min. The China, Australia, and Middle East regions have satellite data every hour. Note that the Australia and China regions are currently covered by MTS1 and the Europe and Africa regions are currently covered by Meteosat-8.

GOES imagers have five bands: visible (0.52-0.71 μm), shortwave infrared (SWIR; 3.73-4.07 μm), water vapor (5.8-7.3 μm), longwave infrared (LWIR; 10.2-11.2 μm), and split window (13.0-13.7 μm). We replaced the water vapor channel, which is not used for cloud detection, with the reflectivity product during the day and the fog product at night (see below and Section 2.1.3 for more details on these products). The spatial resolution of the visible band is 1 km and that

Preferred Site	Latitude (degrees)	Longitude (degrees)	Altitude(km)	Abbreviation
Goldstone, CA	35.25	-116.80	1.10	Gold
Mount Wilson, CA	34.22	-118.06	1.75	Wils
Palomar, CA	33.36	-116.86	1.71	Palo
Table Mountain, CA	34.38	-117.68	2.29	Tabl
Kitt Peak, AZ	31.95	-111.62	2.10	Kitt
White Sands, NM	33.75	-106.37	2.44	Whit
Starfire Optical, NM	34.96	-106.48	1.77	Star
McDonald Obs, TX	30.67	-104.02	2.07	McDo
Mauna Kea, HI	19.83	-155.47	4.27	Maun
Mt. Haleakala, HI	20.71	-156.26	3.05	Hale
Arequipa	-16.47	-71.50	2.45	Areq
La Silla	-29.25	-70.73	2.40	LaSi
Paranal	-24.67	-70.42	2.64	Para
Las Campanas	-29.01	-70.70	2.40	LasC
La Palma	28.77	-17.88	2.30	LaPa
Teide	28.30	-16.51	2.30	Teid
Madrid DSN	40.42	-4.20	0.80	Madr
Calar Alto	37.22	-2.55	2.10	Cala
Gamsberg Table Mntn	-23.27	16.50	2.30	Gams
HESS Telescope	-23.27	16.20	1.80	HESS
Solar Smithsonian	-25.88	17.80	1.60	Sola
S.Africa Astron Tele	-32.38	20.81	1.70	SAAT
Hartebeesthoek	-24.22	27.88	1.40	Hart
Purple Mntn Obs	37.37	97.73	3.20	Purp
Perth Observatory	-31.99	116.14	0.40	Pert
Alice Springs	-22.50	132.50	0.56	Alic
Mt. Stromlo	-34.74	149.01	0.76	MtSt
Anglo/Aust Telescope	-30.74	149.00	1.17	Angl
Canberra DSN	-35.40	149.01	0.67	Canb
Shokin Majdanak Obs	38.72	66.88	1.50	Shok

Table 1: Information about the 30 sites of interest as supplied by JPL. The **Abbreviation** column gives the site name abbreviation used in several figures.
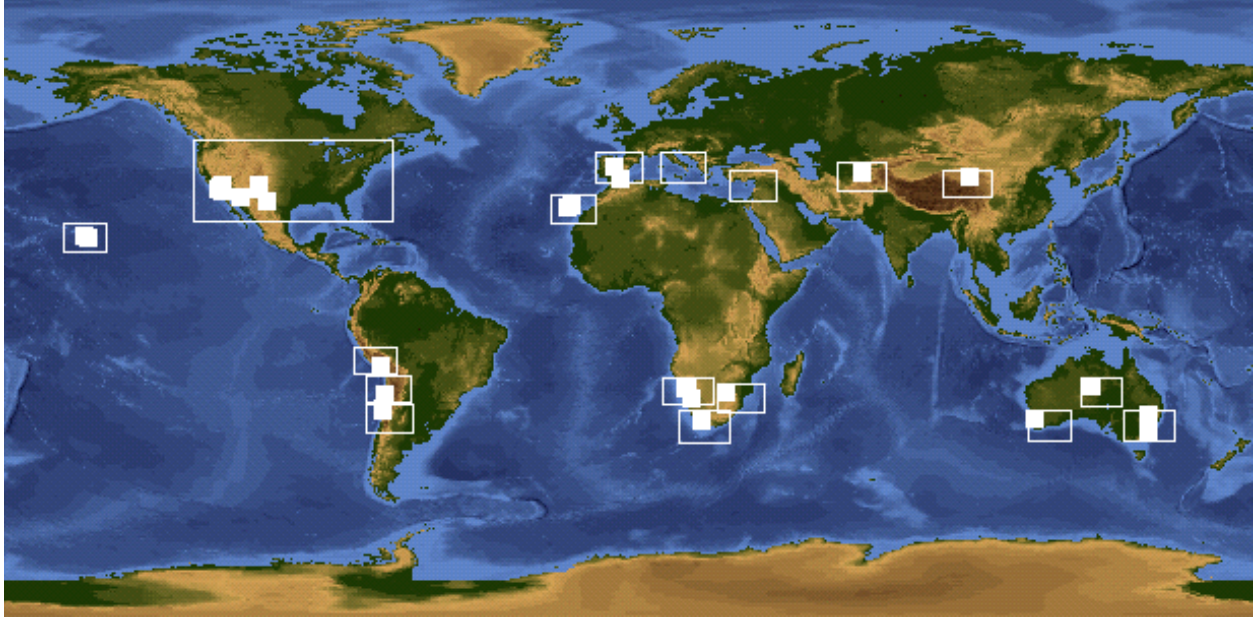
Figure 1: The regions of interest in this study are outlined in the white boxes. The locations of the 30 sites of interest are indicated by the solid white squares. Note that several stations are approximately co-located. See Table 1 for names and locations of these sites.

for the other bands is 4 km. For our purposes, the 1 km data is resampled to 4 km so that it is comparable to the other bands.

During the day, Meteosat imagers provide data in only two bands: visible (0.5-0.7 μm) and LWIR (10.5-12.5 μm) and just one (LWIR) during the night. The spatial resolution is 5 km. The lack of data channels from the Meteosat satellites, in particular, the lack of the SWIR at night, reduces the accuracy of the generated cloud masks. The SWIR is used to calculate the reflectivity product and the fog product. The reflectivity product helps to differentiate between clouds and snow cover during the day and the fog product aids in the detection of fog and low and high clouds at night. With no SWIR data from the Meteosat satellites, these products cannot be generated and the quality of the cloud analysis is reduced. See Section 2.1.3 for more information.

2.1.2. Clear Sky Background

Our cloud analysis techniques for the GOES data are described in detail by Alliss et al. (2000). All cloud tests consist of comparing satellite image values to dynamically computed clear sky background (CSB) values pixel by pixel in the regions of interest. The CSB is discussed below and the main cloud test algorithms (albedo, LWIR, fog, and reflectivity) are discussed in Section 2.1.3.

The CSB is defined as the amount of radiation emitted and/or reflected from a surface that reaches a satellite sensor when no clouds are present. The CSB varies spatially and temporally and is influenced by the radiative properties of the surface material, surface temperature, terrain height, soil moisture, and solar illumination angle. Because of these variations, the CSB must be calculated for each region separately, on a pixel by pixel basis, to generate accurate cloud masks. For example, if the albedo test used a fixed threshold for typical differences between the observed and calculated CSB albedos for all locations, then false cloud detections would be likely over naturally highly reflective regions such as White Sands, NM or the salt flats of northern Chile.

Four CSBs are estimated in the CMG: albedo, reflectivity, LWIR, and fog (Alliss et al. 2004). The CSB is calculated for each pixel by using data from clear times over the 30 previous days at a given analysis time (e.g., 1400 GMT). This approach provides sufficient clear sky data and reduces the effect of diurnal and seasonal cycles of temperature and illumination, in particular, on the calculated CSB. The database from which clear times are determined includes not only the satellite imagery, but also ancillary surface and ship observations collected by the National Weather Service (NWS), World Meteorological Organization (WMO), and several telescope observatories in South America.

The albedo CSB is calculated by identifying the dark-

est 10 % of albedo values from the 30 previous days of visible images. The selected albedo values are averaged to define the CSB for each pixel. The reflectivity CSB is determined only during the day and when snow cover is not likely present. Like the albedo, the darkest 10 % reflectivity product values from the previous 30 days are selected and averaged to generate the reflectivity CSB.

To develop the fog product CSB, the warmest 10 % of LWIR values for the pixel over the previous 30 days are selected. The corresponding fog product values are then averaged to give the fog product CSB. Note that the procedure used to generate the fog product CSB differs from that used to generate the albedo and reflectivity products in which clear pixels are chosen based on the albedo and reflectivity values themselves. Both positive and negative fog product value extremes indicate clouds and the selection of the 10 % warmest and coldest values will not provide the needed information; therefore, the two-step process is used for the fog product CSB.

The LWIR CSB is determined as the average of the difference between the LWIR temperature from the satellite for a given pixel and the LWIR CSB temperature estimated from a linear regression model. The regression model is developed with data from clear sky pixels that are used as prototypes. These prototype pixels are selected by a series of tests that find pixels with a high probability of being clear, even without the benefit of any cloud tests. The coefficients of the regression model for twelve predictors are fit with the data from the prototype pixels. The predictors include satellite data, time, terrain, and regional observations such as cloud cover and air temperature from the NWS and WMO.

The LWIR regression model estimates the clear sky LWIR brightness temperature for each pixel. The LWIR residuals are the differences between the regression model temperatures and the measured imager LWIR temperatures. The warmest 10 % of the LWIR residuals are averaged to determine the LWIR residual CSB that is used in the LWIR cloud tests.

2.1.3. Cloud Tests

The CSB values and the satellite data are compared in four main cloud tests in CMG:

1. LWIR test

2. Albedo product test

3. Fog product test

4. Reflectivity product test.

The LWIR test is applied at all times of the day, unlike the albedo and reflectivity product tests which are applied during the day or fog product tests which are applied at night. A pixel is considered to be cloudy if the LWIR CSB for a given pixel exceeds the LWIR from the satellite by the threshold value or greater. This test cannot easily detect fog and low clouds at night because cloud top temperatures are very similar to surface temperatures. It is unlikely that clouds will radiate in the LWIR at temperatures greater than 300 K. A pixel is deemed clear if the LWIR temperature is greater than 300 K, even if the LWIR cloud test indicates that it is cloudy.

The fog product is used to detect low clouds and fog at night. The fog product test is a multi-spectral test that compares values of the fog product calculated as the difference between the LWIR and the SWIR brightness temperatures (Ellrod 1995). The temperature differences result mainly because clouds observed in the SWIR have an emissivity that is 20 % - 40 % lower than clouds observed in the LWIR (Hunt 1973). Therefore, at night, liquid stratiform (low) clouds appear colder in the SWIR than they do in the LWIR. Typical $T_{LWIR} - T_{SWIR}$ for fog and low stratus are approximately 2 K or larger (Lee et al. 1997). The fog product can also detect ice clouds, which are highly transmissive and therefore, appear warmer in the SWIR. Typical $T_{LWIR} - T_{SWIR}$ values for ice clouds are approximately -5 K or lower. The daytime SWIR is dominated by reflected solar SWIR and therefore, the fog product is only useful at night.

The albedo test, which uses visible data, is applied when the solar zenith angle is below $89°$. This test detects clouds if the pixel is more reflective than the albedo CSB and the difference is greater than a predefined threshold for that pixel. If the difference between the calculated albedo and the CSB is less than the threshold, the pixel is deemed clear.

The albedo test may falsely detect snow as clouds. Therefore, the shortwave reflectivity product is implemented during the day to decide if a pixel is cloudy or if the surface is snow-covered. This product indicates the amount of reflected solar SWIR detected and is derived by removing the thermal component from the SWIR (Allen et al. 1990, Setvák and Doswell 1991). Water clouds are highly reflective in the SWIR while ice clouds are poorly reflective in the SWIR. As a result, water clouds appear as bright white and poorly reflective ice clouds and snow appear as dark gray or black in the resulting images. The reflectivity product, then, can easily distinguish between low clouds and snow cover. The reflectivity test is only applied when and where snow cover is likely and can override a false cloud detection for snow cover indicated by the albedo

test. To ensure that high ice clouds (which also appear dark in the reflectivity test) are not present, the LWIR test also must not indicate the presence of high clouds for a pixel to be considered clear.

Meteosat-5 and Meteosat-7 provide only LWIR data at night and only visible and LWIR data during the day. The lack of a SWIR band from these two satellites limits the accuracy of the cloud masks. At night, with no SWIR, there is no fog product with which to detect low clouds or fog. During the day, there is no reflectivity product and so it is possible that false detection of snow as clouds from the albedo test may occur, resulting in less accurate cloud masks.

With the CSB and satellite data, the CMG performs the necessary tests to determine the cloud masks. During the day, for example, over southern Italy and Sicily, LWIR and albedo products are used to detect clouds with the resulting mask accurately showing the location of clouds (Fig. 2). At night when low clouds cannot adequately be detected by the LWIR, the fog product is vital to developing accurate cloud masks. In fact, in a cloud scene from southwestern Australia (Fig. 3), the low clouds over the land would not have been detected without the fog product.

Because of the extensive development, testing, and validation of CMG by TASC, we believe the cloud masks are very accurate. However, in the course of this investigation, we encountered two problems with the cloud mask analysis that require further investigations to correct. First, in several of the worldwide regions, in particular China and Namibia, there is insufficient WMO surface observation data for CMG to properly generate the LWIR CSB. As a result, there are many false detections in these regions (Fig. 4). We augmented parts of the CMG code to reduce some of the false detections. To resolve this issue more completely, more surface data sources for these regions must be identified and used in CMG.

The second issue that must be resolved is under-detection of low clouds over land in humid environments such as southwestern Australia (Fig. 5). The underdetection most likely results because the cloud top temperatures are very similar to the underlying ground temperatures. A more thorough investigation must be performed to develop solutions for this issue.

2.2. Lasercom Network Optimization Tool

The goal of optimization in developing a network of ground stations for optical communications is to achieve the highest availability for the network, i.e., the greatest percentage of time during which at least one ground station can communicate with the probe, with the fewest number of stations in the network. Not only must the cloud fractions at each site be considered, but also station locations with respect to one another must be considered. Selecting stations all in the same area, say within several hundred kilometers of one another, will result in low availabilities. In such a case, the low availabilities result because the stations could not see the probe a large percentage of the time due to the probe's movement with respect to the earth. If stations whose cloud patterns are highly correlated are selected, the availability may also be reduced because when one station is cloudy and thus unavailable, one or more of the other stations are likely to be the same. Geographically diverse stations will tend to be less correlated and because they would be positioned over a wide region of the globe, availability would be expected to be higher than the scenarios outlined above.

The process of finding an optimal ground station network is a discrete optimization problem. With over 420,000 pixels in TASC's cloud database for the regions considered in this study, the search space must be reduced to be practical. JPL provides some constraints on the locations of stations:

1. Stations must be within $\pm 41°$ latitude

2. Elevation angle of the probe with respect to the station must be greater than $20°$ for each pixel to be considered

3. Minimum station altitudes of 0 km, 1 km, 1.5 km, or 2 km

4. Stations must be selected from a list of sites of interest (Table 1).

Even with these constraints, the database is too large to search exhaustively for the network with the maximum availability. Therefore, the optimization algorithm must be able to find the desired networks by searching only a small fraction of the network configuration space.

The optimization process we employ in LNOT, a downhill simplex method (Press et al. 1994), seeks a balance between what we call *locality* and *robustness*. Locality refers to the idea that good network configurations are close together in space. This feature lets the algorithm make progress in selecting stations. If we did not have the locality feature, the nth guess would be no better than the first guess. On the other hand, it is desirable that the algorithm not get trapped in local extrema in the configuration space. This feature is known as robustness. Our optimization process represents a trade-off between locality and robustness in two distinct stages. In the first stage, the algorithm searches widely over the entire configuration space, sacrificing
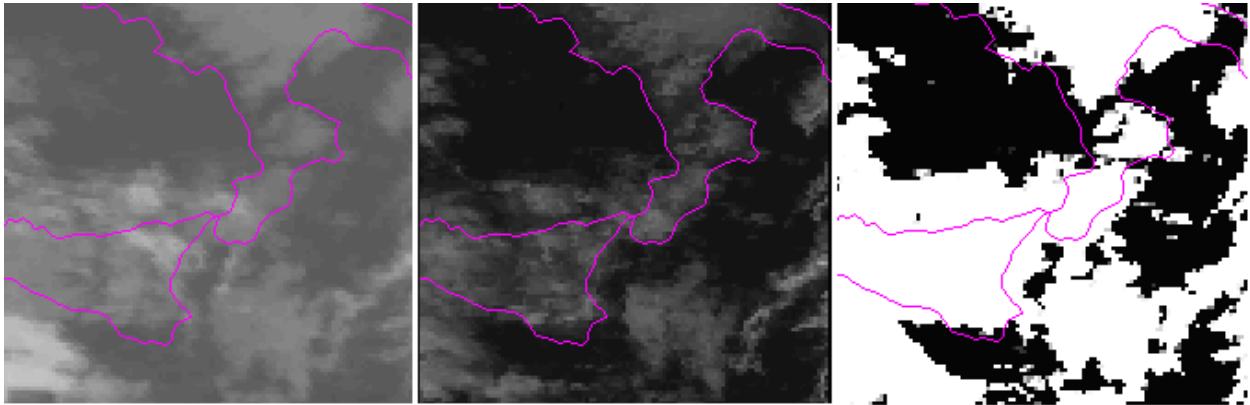
Figure 2: A sample cloud scene during the day for southern Italy and Sicily. The image on the left is the LWIR image from Meteosat-7. The image in the center is the corresponding visible image from Meteosat-7. For these two images, the lighter gray areas indicate clouds. The cloud mask on the right shows clouds as white and was generated with CMG.
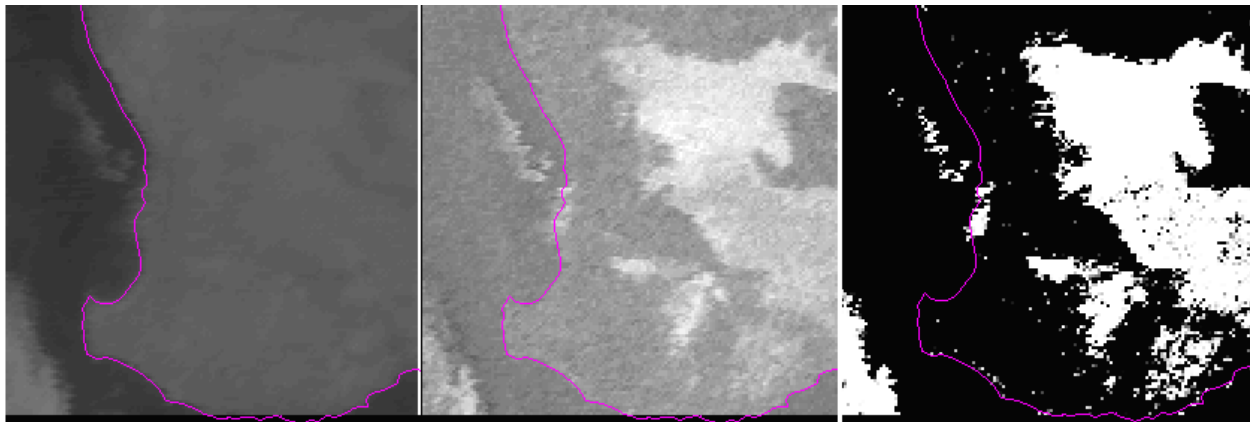
Figure 3: A sample cloud scene during the night for southwestern Australia. The image on the left is the LWIR image from GOES-9. Note the small area of clouds in the southwestern corner over water. The image in the center is the corresponding fog product calculated from data provided by GOES-9. Note the large area of fog in the lighter gray and white shades over the land. The cloud mask on the right shows clouds as white and was generated with CMG.
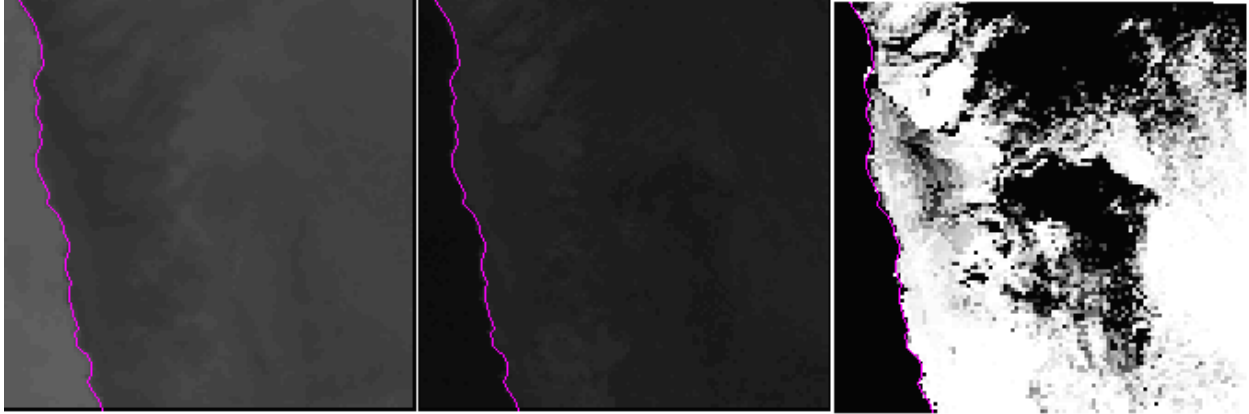
Figure 4: A sample cloud scene during the day for Namibia. The image on left is the LWIR image from Meteosat-7. The image in the center is the corresponding visible from Meteosat-7. These images show that this tile is essentially clear at this time. However, the mask on the far right shows considerable false detections.
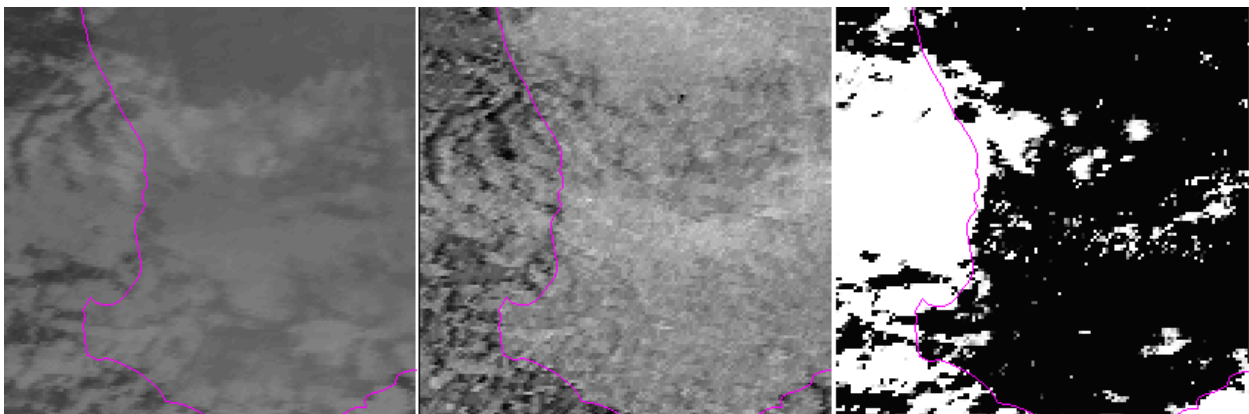
Figure 5: A sample cloud scene during the night for southwestern Australia. The image on left is the LWIR image from GOES-9. The image in the center is the corresponding fog product. These images show substantial cloud cover over the land and ocean. However, the mask on the far right does not indicate many clouds over land.

some locality in favor of robustness. Once the algorithm arrives in the vicinity of the solution, the second stage begins. In the second stage, some robustness is sacrificed in favor of locality as the algorithm finds the best configuration in the neighborhood of the last configuration found by the first stage. The limited robustness found in the second stage is not of concern because we assume that the optimal solution is nearby when we begin the second stage.

A typical optimization run evaluates more than 40 million networks. At the end of the optimization process, we further evaluate the availabilities of the ten best networks found by considering detailed line of sight calculations that take into account ground station locations, effects of parallax between the satellite imager and the probe, the elevation angle of the probe, and cloud amount in a 2400 km^2 area centered on each station. To make these calculations, the position of the probe with time must be known. We assume that the probe has a circular orbit that is at $0°$ inclination to the ecliptic, with a radius of 1.5237 AU (Astronomical Units; 1 AU= 149,597,870 km). This orbit is similar to that of Mars and is much faster to calculate than an elliptical, inclined orbit.

2.3. Experiments

We present single site CFLOS results for the sites of interest (Table 1; Fig. 1) for June 2003 through May 2004. We also generated network availabilities for two different experimental designs: Restricted and Unrestricted for this time period. In the restricted runs, the only sites that are considered by LNOT are those from the sites of interest. These sites were chosen because they currently have infrastructure with which to build laser communication facilities. They are also distributed around the globe at somewhat regular longitudinal intervals, possibly allowing some of these sites to be used in a linearly dispersed optical subnet (LDOS) network configuration. Note that at present, NASA/JPL has not secured agreements to actually use some of these sites. We computed availabilities for a probe in southern (Fig. 6) and northern (Fig. 7) declinations to compare networks for these two extreme scenarios. Note that for the southern declination, the probe is over the southern hemisphere 75 % of the time, while for the northern declination, the probe is over the northern hemisphere 100 % of the time.

For the unrestricted runs, we allow LNOT to consider any pixel over land in the regions of interest. We allowed LNOT to consider sites at or above 0 km, 1 km, 1.5 km, and 2 km. We computed availabilities for a probe in northern and southern declination.

3. RESULTS

3.1. CFLOS for the Sites of Interest

For the period of June 2003–May 2004, Las Campanas and La Silla had the highest CFLOS values from the sites of interest with CFLOS values around 81 % (Fig. 8; Fig. 9). Purple Mountain had the lowest value of 37 %. When examined by region, the highest CFLOS values came from the South America regions with an average CFLOS over four sites of about 74 %. The sites in Spain had the lowest regional average of about 46 %.

3.2. Network Statistics

The period of record, June 2003–May2004 is shorter than the 18 month period of the Mars probe orbit. Therefore, the networks developed do not consider a complete probe orbit. Moreover, the one year database cannot adequately capture the longer term changes in atmospheric circulation such as El Niño/La Niña. Several years of cloud data are needed to ensure fidelity of network statistics.

3.2.1. General Features of Restricted and Unrestricted Networks

In general, as the number of stations in the restricted and unrestricted networks increases, the availability increases for networks generated when the probe is in southern and northern declinations (Fig. 10; Fig. 11). To attain a network availability of 90 % or greater with the probe in southern declination, six sites from the restricted runs are needed. For the unrestricted runs considering stations at or above 0 km, five sites are needed, while for stations at or above 1 km, six sites are needed. Nine stations are needed when the minimum station altitude is 1.5 km. Note that increasing the network size beyond seven sites does not result in substantial increases in availabilities. With the 2 km altitude restriction in the unrestricted runs, 90 % availability is never reached because of the limited number of pixels over which to optimize. Moreover, with the 11 and 12 site unrestricted 2 km networks, there are not enough pixels over which to search and optimize and therefore, these networks are not developed. Availabilities of up to 99 % are generated for the 12 site restricted runs.

When the probe is in its northern declination phase, six sites for the restricted networks and five sites for the 0 km unrestricted runs are needed to meet the 90 % availability benchmark, consistent with the southern declination networks. However, the benchmark is reached with only five sites with the 1.5 km unrestricted
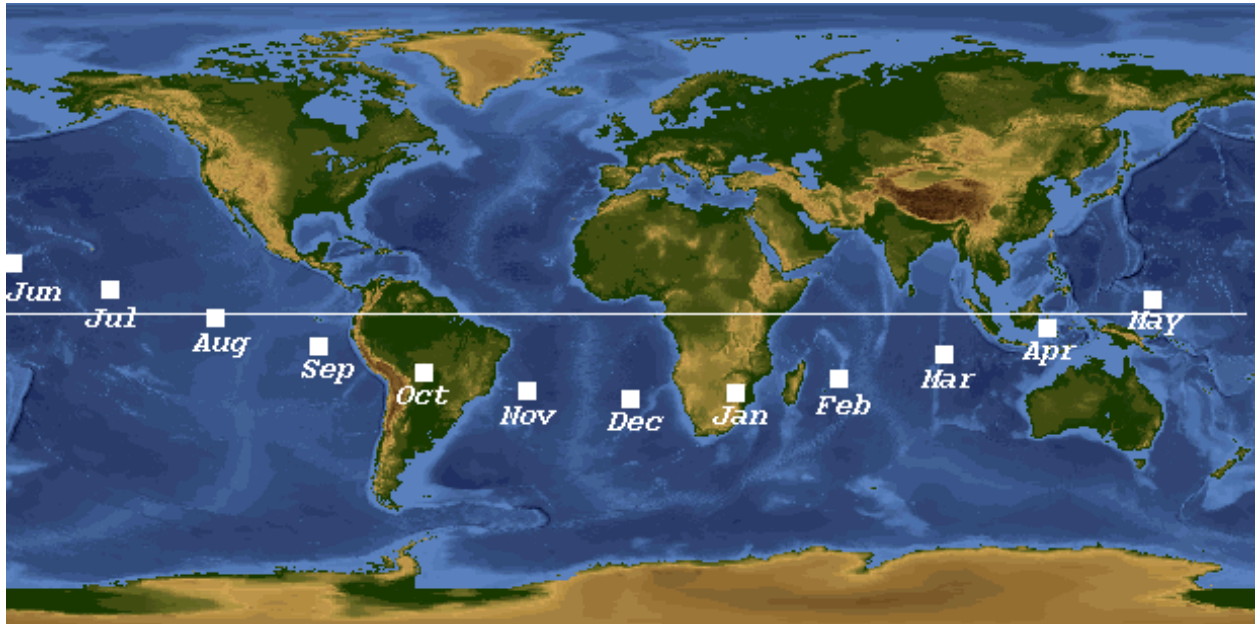
Figure 6: Probe locations, indicated by the white squares, at 23:45 UTC on the last day of the month from June 2003 – May 2004 for the southern declination analysis. The white line indicates the equator.
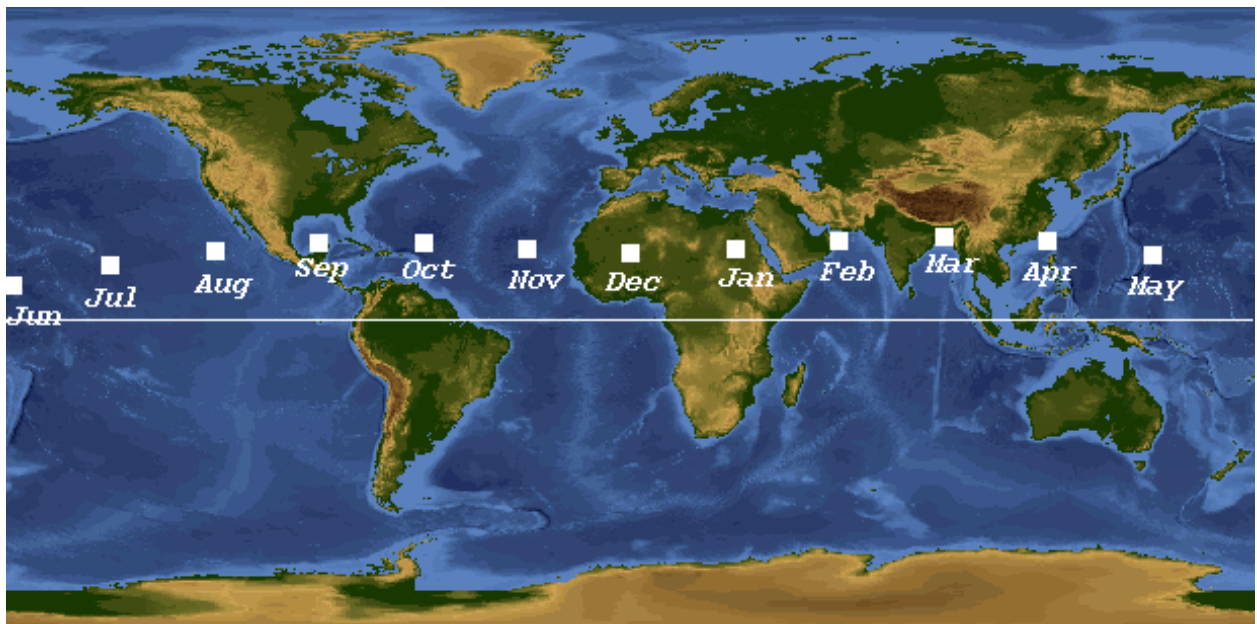
Figure 7: Probe locations, indicated by the white squares, at 23:45 UTC on the last day of the month from June 2003 – May 2004 for the northern declination analysis. The white line indicates the equator.
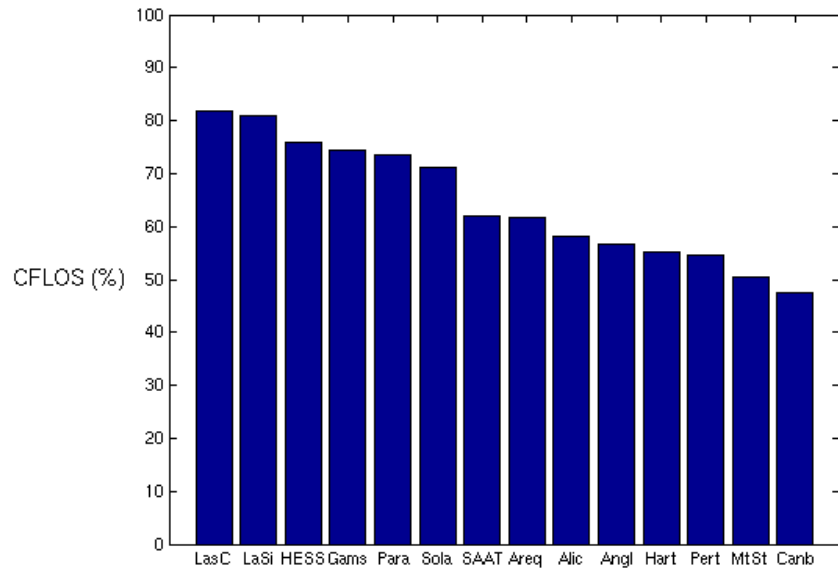
Figure 8: CFLOS values for June 2003–May 2004 for the sites of interest in the southern hemisphere. See Table 1 to match the abbreviated site names used in this figure to the sites of interest.
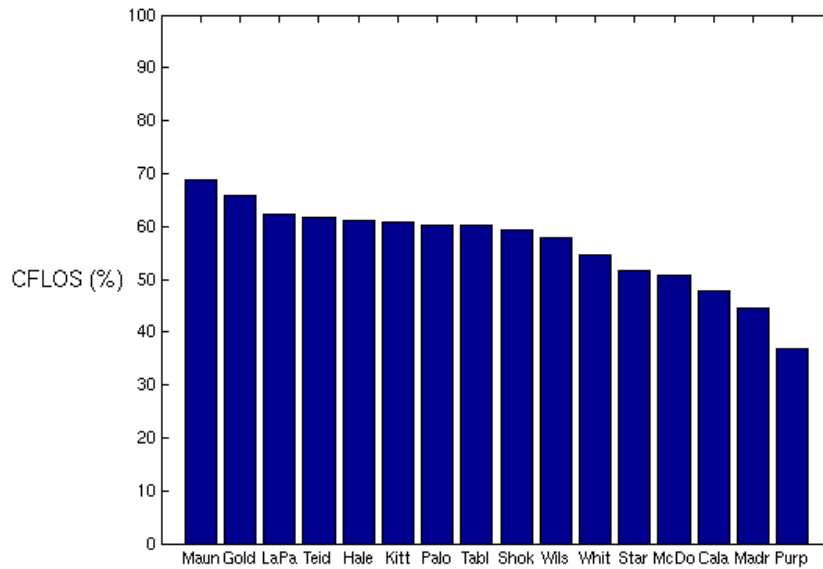
Figure 9: CFLOS values for June 2003–May 2004 for the sites of interest in the northern hemisphere. See Table 1 to match the abbreviated site names used in this figure to the sites of interest.

runs and six sites with the 2 km unrestricted runs for which the availabilities are much higher than their counterparts from the southern declination runs. The highest coverage rates are found over northern hemisphere pixels when the probe is in northern declination. Moreover, most pixels at or above 1.5 km are located in the northern hemisphere. Both of these facts contribute to higher availabilities and smaller network sizes needed to attain 90 % for the higher altitude networks when the probe is in northern declination.

More stations are required to achieve the desired availability as the minimum station altitude increases (Fig. 10; Fig. 11). As the altitude increases, LNOT has fewer pixels over which to optimize. In addition, higher altitude locations may experience greater cloud cover than lower altitudes. This dependence is less dramatic for the northern declination data than for the southern declination data, perhaps the result of better coverage for the northern hemisphere where most of the higher elevations are located.

3.2.2. Restricted Networks

A network size of 6 sites or more is needed to reach a network availability of 90 % or greater for the restricted runs when the probe is at southern declination (Fig. 10). For the six site network, the availability during the period of record is 91%. In this network, five of the stations are located in the southern hemisphere, in southern Chile, Namibia, and Australia (Fig. 12). The remaining station is in California. During this time period, the Mars probe provides increased coverage to the southern hemisphere sites of interest, resulting in the selection of more southern hemisphere sites. Also, the Australia sites are in a good location geographically for optical stations.

Note that the sites in the six site network as chosen by LNOT show features of an LDOS configuration. The sites in this network are distributed around the globe at somewhat regular intervals. Moreover, for some of the larger networks, the sites are clustered in southern Africa, Chile, and Australia.

When the probe is forced into a northern declination, again six sites are needed to get an availability of 90 % or greater (Fig. 11). This network has four sites in the southern hemisphere and two in the northern hemisphere (Fig. 13), whereas the southern declination network had just one station in the northern hemisphere. The greater coverage of the northern hemisphere stations in the northern declination runs produces higher availabilities and more northern hemisphere stations.

Networks of six sites or more often contain more than one station in southern Africa, Chile, and Australia. Note that Goldstone, HESS Telescope, and Perth Observatory were selected for both the northern and southern declination experiments.

3.2.3. Unrestricted Networks

For the unrestricted southern declination LNOT runs with an altitude restriction of 0 km, five sites are needed for an availability of 90 % or greater (Fig. 10). This network contains two stations in the northern hemisphere and three in the southern hemisphere (Fig. 14). The stations selected are in California, Chile, and Australia, as seen in the restricted runs, but a location in the Israel tile was also selected. For other five site networks with slightly lower availabilities than the one discussed above, stations in Chile, Yemen, and central Australia were frequently present.

For networks with stations at 1 km or above, six sites are needed to achieve a 90 % availability (Fig. 10), with the stations evenly divided between the northern and southern hemisphere (Fig. 15). Stations in California, Chile, and Australia are once again chosen. However, two stations from the Middle East are also selected.

The networks composed of stations at 1.5 km or above need at least nine sites to reach 90 % availability (Fig. 10). As the minimum altitude increases, the number of pixels that are considered in LNOT's optimization is reduced. As a result, it takes more pixels to attain the availability goal. Also, more of the searchable pixels are from the northern hemisphere as the minimum altitude increases since much of the area at or above 1.5 km in our regions of interest is in the northern hemisphere. The result is eight stations located in the northern hemisphere and only one in the southern hemisphere (Fig. 16) even though the probe is in southern declination. Note the evidence of some clustering as two stations are selected in California and China.

When the probe is in northern declination for the 0 km runs, there are three southern hemisphere stations and two northern hemisphere stations (Fig. 17). There are more stations in the northern hemisphere for these networks than in the southern hemisphere for the unrestricted 1 km, 1.5 km, and 2 km networks (Fig. 18; Fig. 19; Fig. 20). A station in northern Chile is found in most networks. For networks with availabilities above 90 %, most of the sites are in southwestern CONUS, Hawaii, and the Middle East. For the higher altitude runs, China sites are added as the network size increases. For the lower altitude runs, sites in Australia and southern Africa are added to the network as the network size increases. This fact suggests that the more favorable sites are located in the southern Africa and Australia, but these are not considered for networks in the higher altitude runs. Note that when the
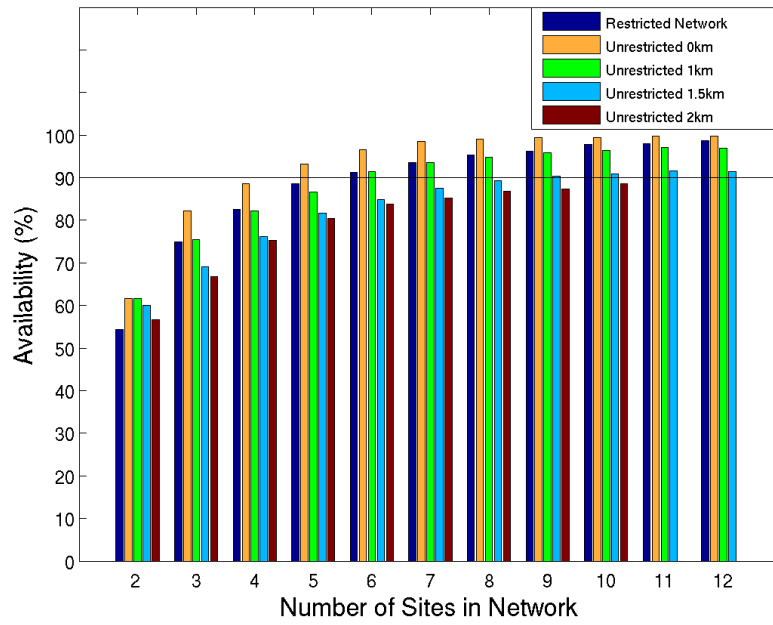
Figure 10: Availabilities for 2 to 12 station networks for June 2003 – May 2004 when the probe is its southern declination.
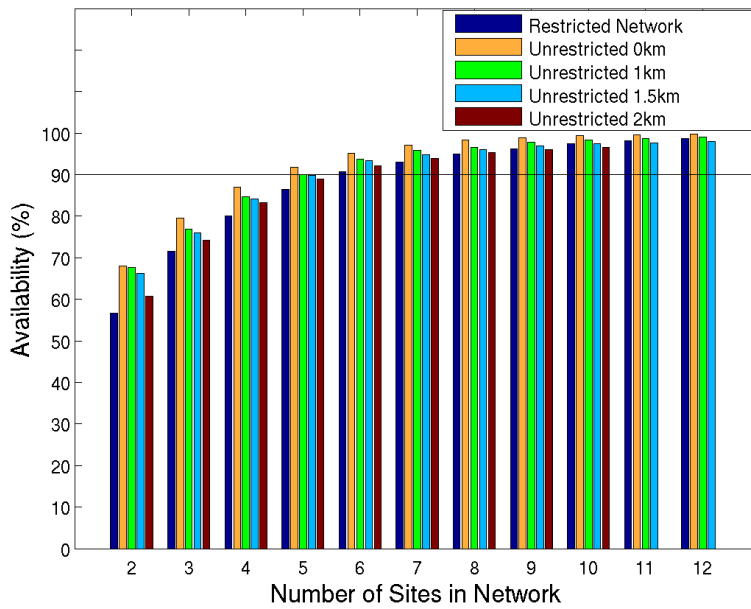
Figure 11: Availabilities for 2 to 12 station networks for June 2003 – May 2004 when the probe is in its northern declination.
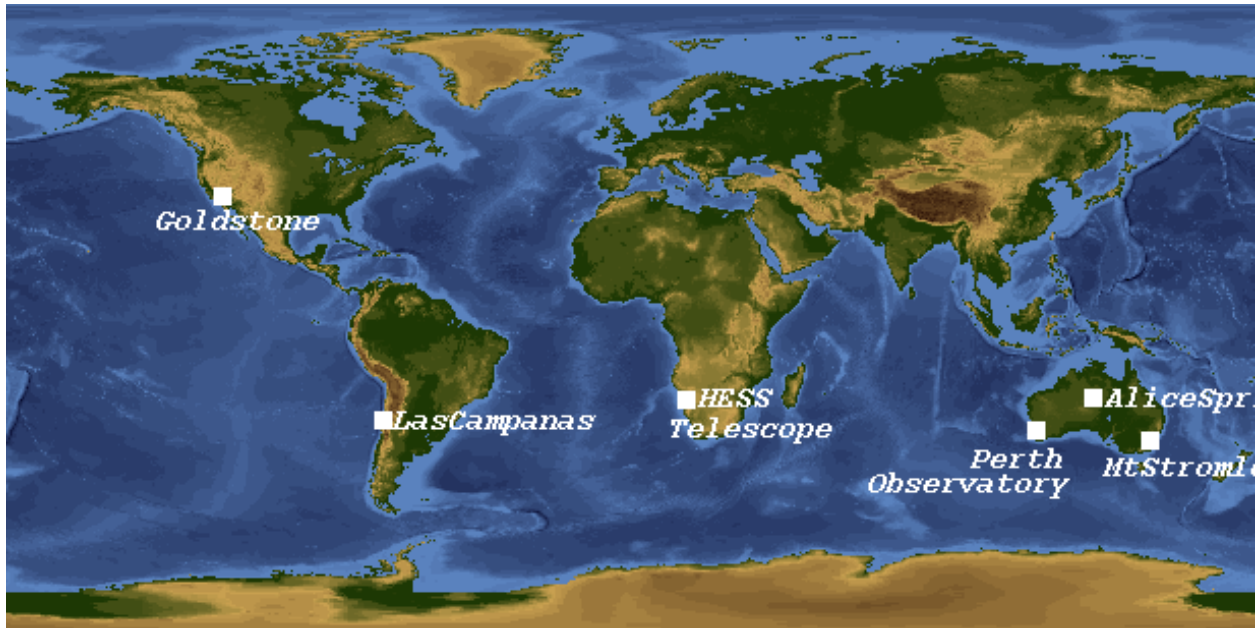
Figure 12: Locations of stations in the first restricted network reaching at least 90 % availability when the probe is at southern declination. These sites were selected by LNOT from the sites of interest and with data from June 2003 – May 2004. The availability of this network is 91 %.
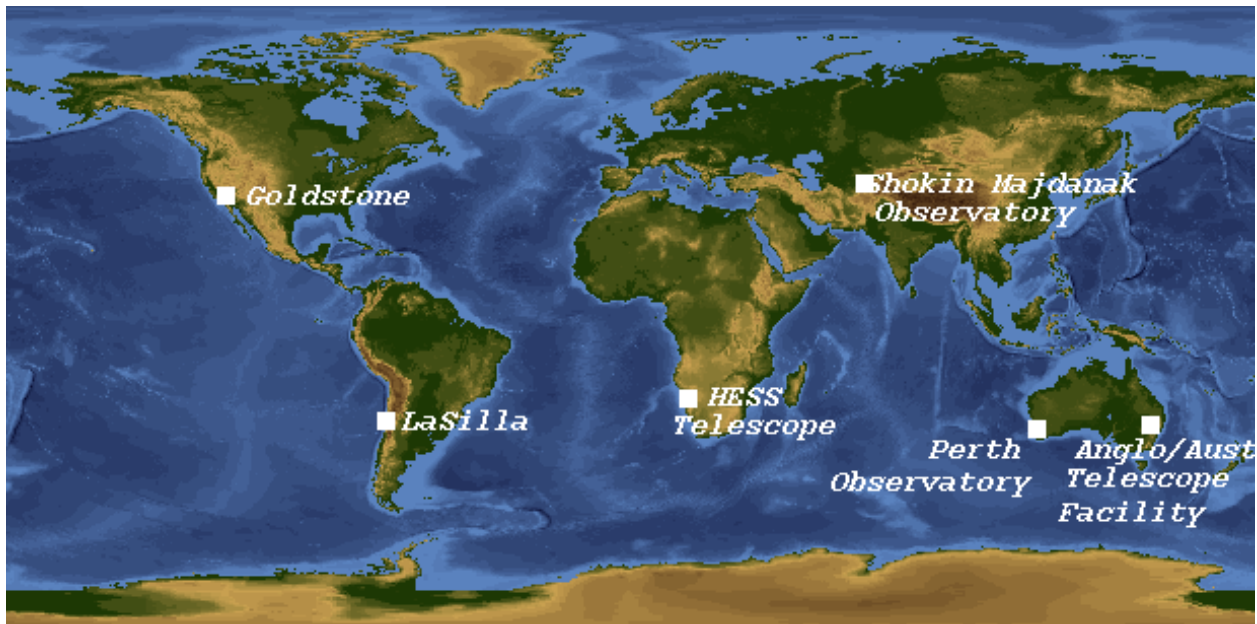
Figure 13: Locations of stations in the first restricted network reaching at least 90 % availability when the probe is at northern declination. These sites were selected by LNOT from the sites of interest and with data from June 2003 – May 2004. The availability of this network is 91 %.
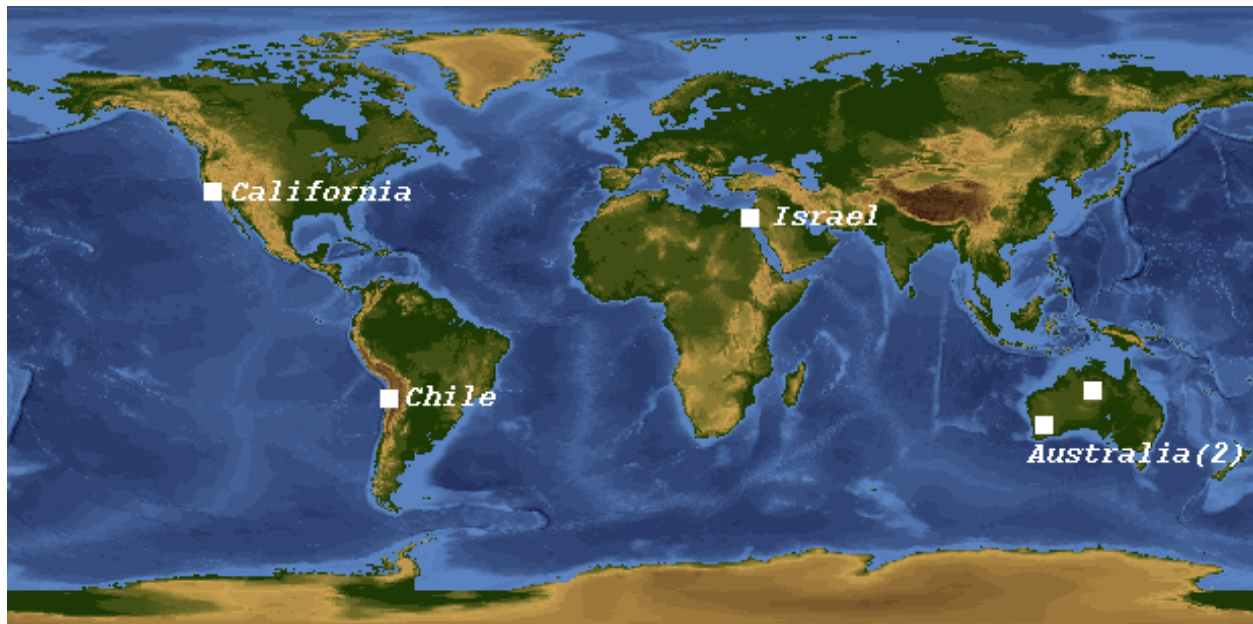
Figure 14: Locations of stations in the first unrestricted network reaching at least 90 % availability when the probe is at southern declination. These sites are at a minimum altitude of 0 km and were selected by LNOT with data from June 2003 – May 2004. The availability of this network is 93 %.

probe is in its northern declination, the networks from the 2 km unrestricted runs reach 90 % availability with six sites. Recall that with the southern declination, the 2 km networks never reached 90 %. The probe is in a better position for the northern hemisphere high altitude regions when it is in the northern declination. As a result, the availability increases substantially.

3.2.4. Station Substitution Studies

LNOT is implemented to find the optimal networks by optimizing over network availability. When ground station locations are chosen for development, however, other factors, such as funding or site accessibility, must be considered. It is possible that one station in an optimized network may be unsuitable for use in a network but that another nearby station is more practical. Therefore, in this section, we examine the effects of substituting one station in a network with another station on the network availability.

The network we use as the base for these studies is the first southern declination restricted network to reach 90 % availability or higher (Fig. 12). All of the substitutions we made cause the availability to remain the same or decrease, as would be expected since the base network is the optimal network determined by LNOT. When Goldstone is replaced with Palomar, Table Mountain, or Kitt Peak (all within about 210 km of Goldstone), the change in the network availabilities is

negligible as networks with any of these stations have availabilities of 91 % (Table 2). Therefore, for these stations, there is some flexibility in choosing a station in this region. When Goldstone is replaced with stations that are further away, such as Starfire or White Sands in New Mexico (both about 950 km from Goldstone), the availability drops to approximately 89 %. The largest change in network availability from the substitutions that we examined occurs when replacing HESS with South Africa Astronomical Telescope, stations that are more than 1100 km apart. The availability of the network drops to 87 %. A network containing all three of Deep Space Network (DSN) stations is obtained by replacing Perth Observatory with Madrid DSN and Mt. Stromlo with Canberra DSN. The availability of this network is approximately 89 %.

4. SUMMARY

Laser communications between ground stations and space-borne probes can be interrupted by clouds. To mitigate the effects of clouds and to attain high availability of the communication link between the ground and a probe, a geographically diverse network of ground stations is needed. The stations in this network should have limited correlation with one another and should be placed so that there is overlap betweens stations as the probe rises and sets every day. With such a network, if one station is cloudy or does not have coverage
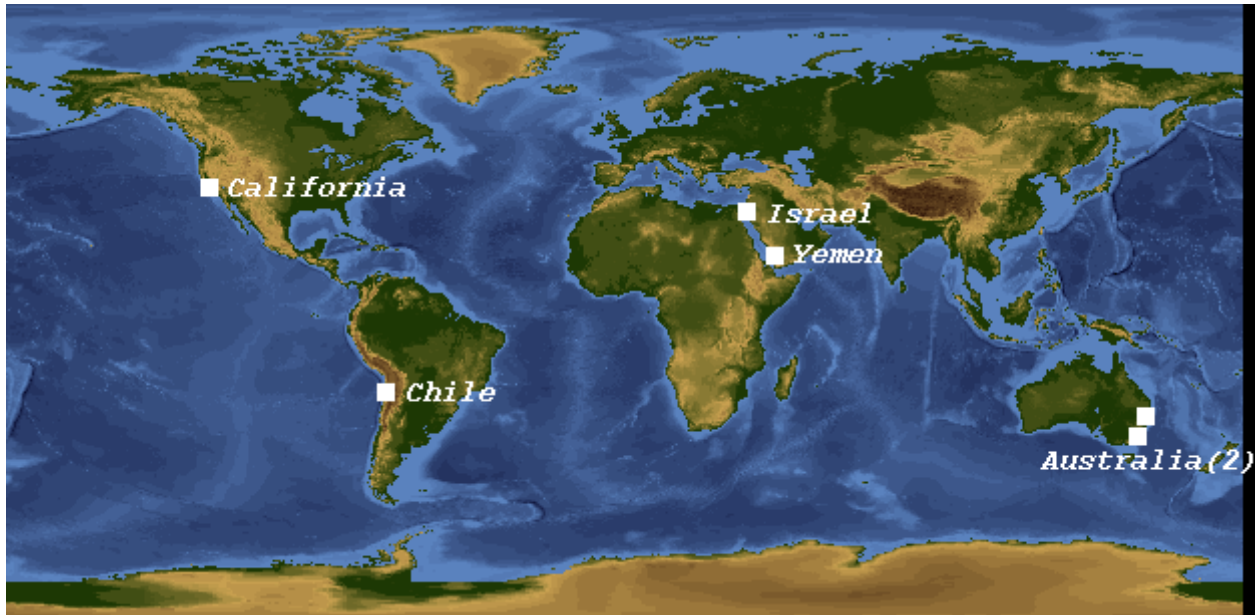
Figure 15: Locations of stations in the first unrestricted network reaching at least 90 % availability when the probe is at southern declination. These sites are at a minimum altitude of 1 km. and were selected by LNOT with data from June 2003 – May 2004. The availability of this network is 90 %.
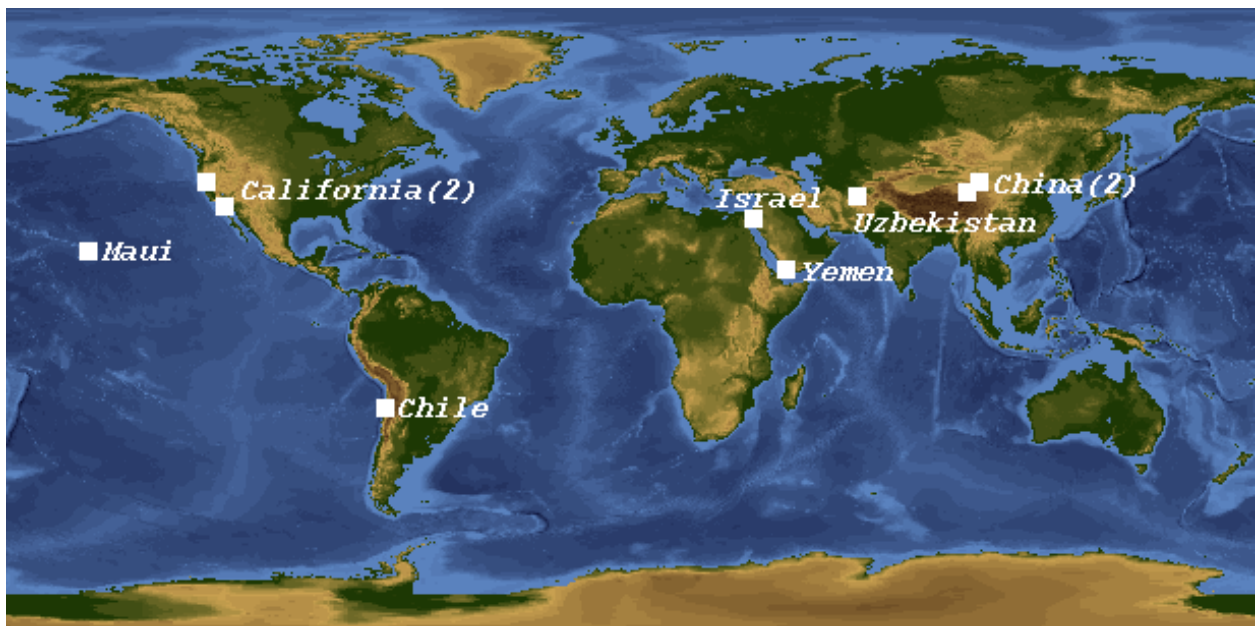
Figure 16: Locations of stations in the first unrestricted network reaching at least 90 % availability when the probe is at southern declination. These sites are at a minimum altitude of 1.5 km and were selected by LNOT with data from June 2003 – May 2004. The availability is 91 %.
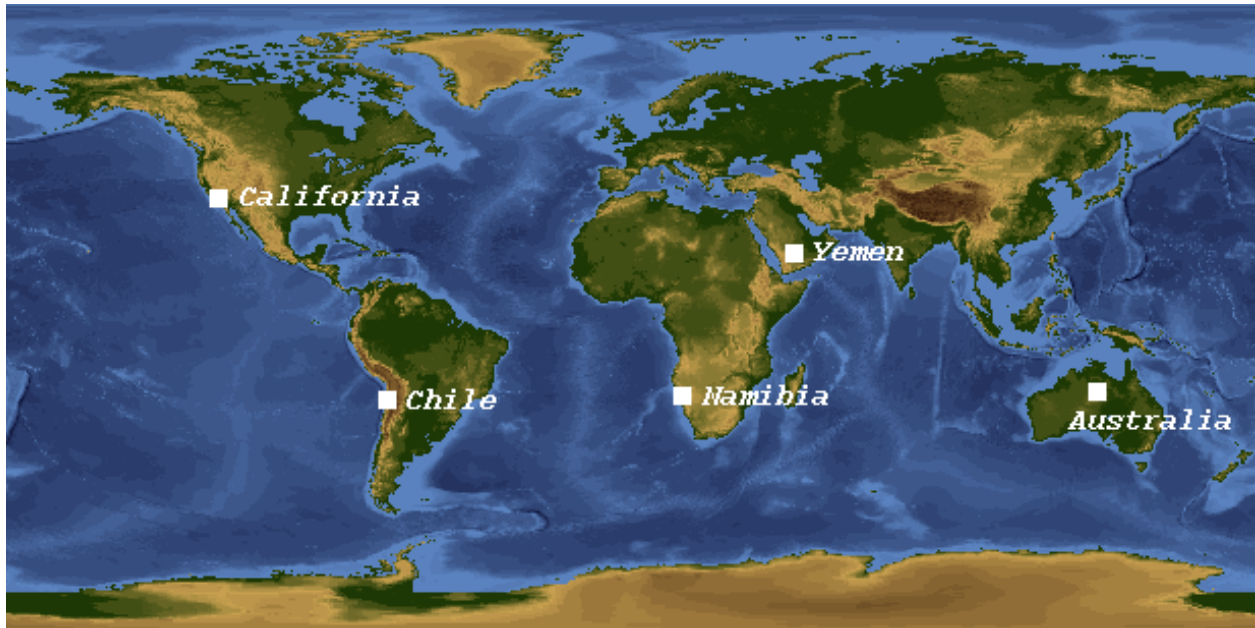
Figure 17: Locations of stations in the first unrestricted network reaching at least 90 % availability when the probe is at northern declination. These sites are at a minimum altitude of 0 km and were selected by LNOT with data from June 2003 – May 2004. The availability of this network is 92 %.
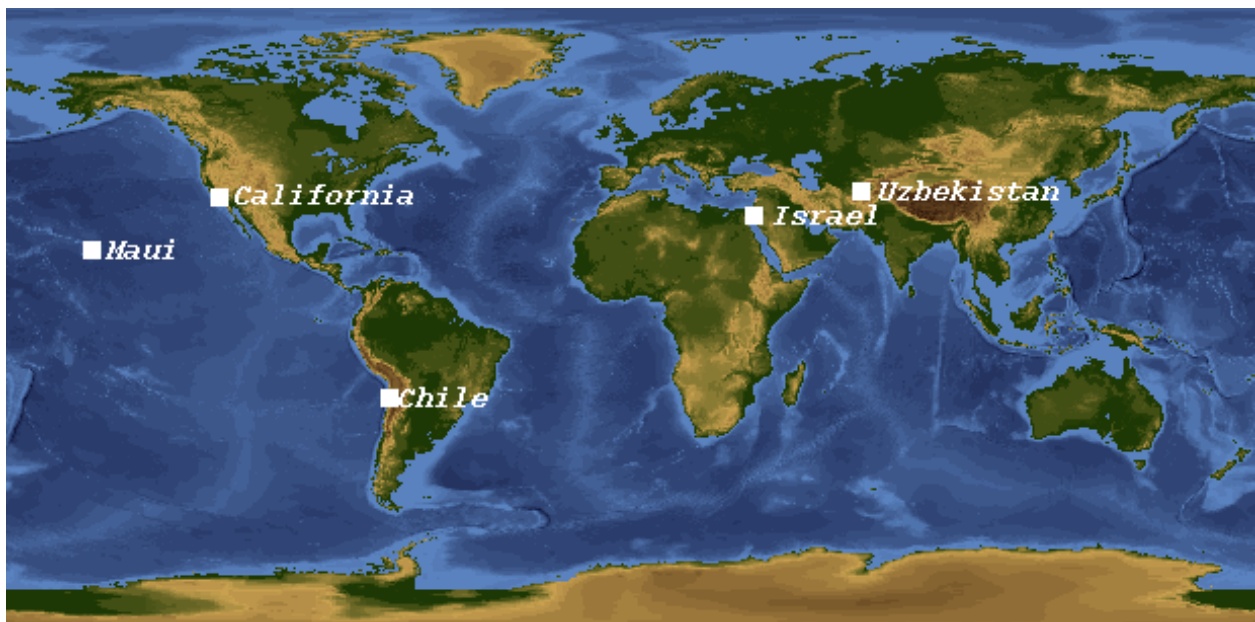
Figure 18: Locations of stations in the first unrestricted network reaching at least 90 % availability when the probe is at northern declination. These sites are at a minimum altitude of 1 km and were selected by LNOT with data from June 2003 – May 2004. The availability of this network is 90 %.
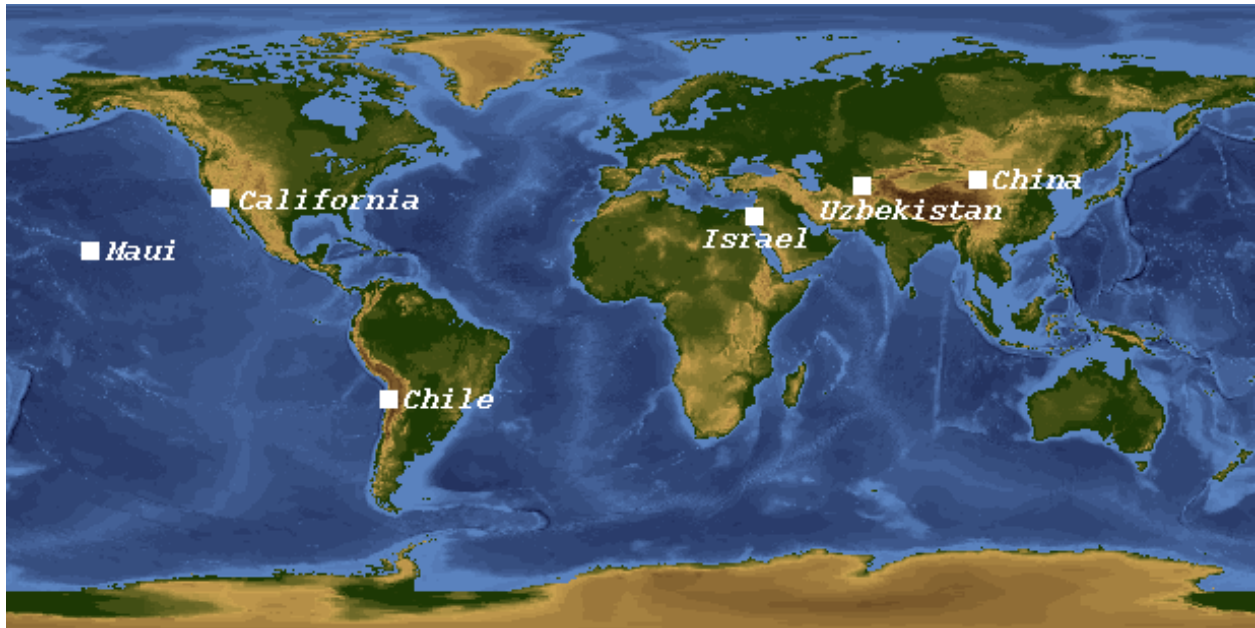
Figure 19: Locations of stations in the first unrestricted network reaching at least 90 % availability when the probe is at northern declination. These sites are at a minimum altitude of 1.5 km and were selected by LNOT with data from June 2003 – May 2004. The availability of this network is 93 %.
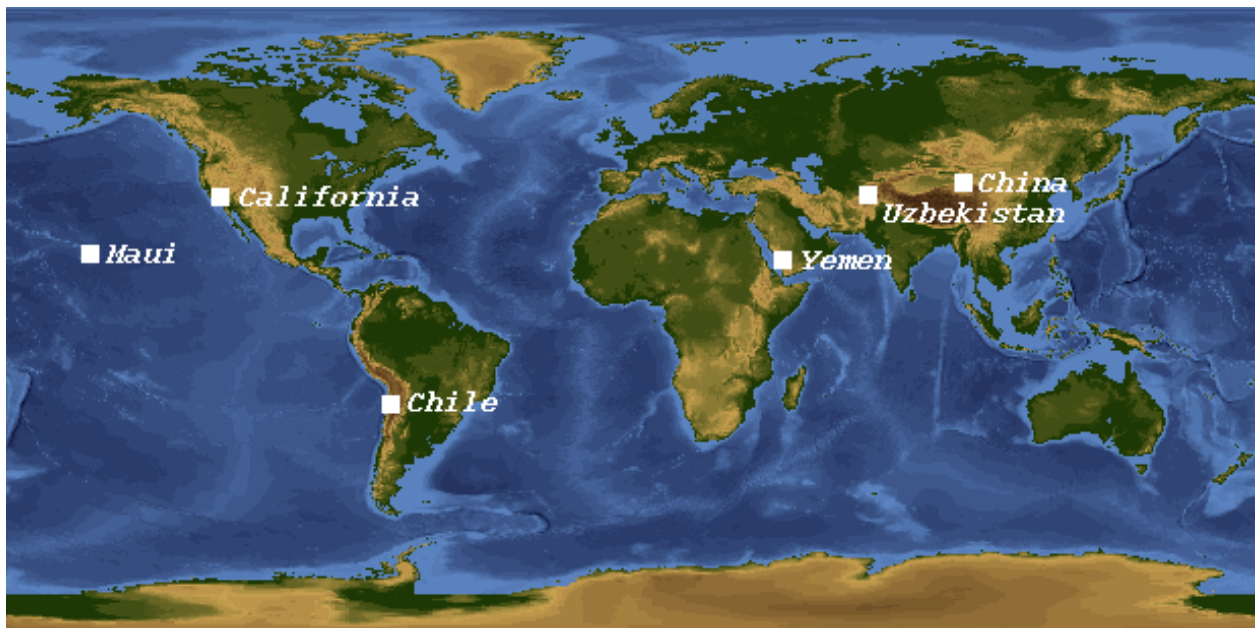
Figure 20: Locations of stations in the first unrestricted network reaching at least 90 % availability when the probe is at northern declination. These sites are at a minimum altitude of 2 km and were selected by LNOT with data from June 2003 – May 2004. The availability of this network is 92 %.

Optimal Network:	Availability
Goldstone, CA Las Campanas Perth Observatory Alice Springs Mt. Stromlo HESS Telescope	91.2%
Replaced Goldstone, CA with Palomar, CA	91.2%
Replaced Goldstone, CA with Table Mountain, CA	90.7%
Replaced Goldstone, CA with Kitt Peak, AZ	91.2%
Replaced Goldstone, CA with Starfire Optical Range, NM	88.5%
Replaced Goldstone, CA with White Sands, NM	88.9%
Replaced Perth Observatory with Calar Alto	89.2%
Replaced Perth Observatory with La Palma	89.5%
Replaced HESS Telescope with S.Africa Astron Telescope	87.3%
Replaced HESS Telescope with Solar Smithsonian	90.7%
Replaced Las Campanas with La Silla	91.1%
Replaced Perth Observatory with Madrid DSN and Replaced Mt. Stromlo with Canberra DSN	88.8%

Table 2: Network availabilities for the station substitution experiments. The optimal network is the first southern declination restricted network to reach 90 % availability (Fig. 12).

of the probe, another station is available to use in its place.

The determination of these ground station networks requires cloud climatologies and an optimization algorithm that considers cloud cover and the position of a probe with respect to the ground stations. LNOT, in-house software that selects networks of stations with optimal availabilities, has been applied to the problem of finding networks that can communicate with a probe in approximate Mars orbit with an availability of 90 % or greater. The regions of interest for which we have begun developing cloud climatologies are CONUS, Hawaii, South America, Europe, northern Africa, southern Africa, the Middle East, central and eastern Asia, and Australia.

In many cases, a network with an availability of 90 % or greater can be obtained with five or six sites. Increasing the number of sites beyond seven sites results in only small gains in availability. The optimal networks chosen by LNOT contain stations that are spaced at somewhat even intervals across the globe, similar to an LDOS configuration. By adding more stations in areas already selected, LNOT is able to increase the availabilities even further. However, when we created LDOS and COS networks (not shown) from the sites of interest (non-optimized networks), eight or more stations were required to reach an availability of 90 % or greater. Therefore, selecting a network through optimization with LNOT produces a ground station network that can reach the target availability with fewer stations than would be needed by traditional LDOS and COS networks.

Stations in southwestern CONUS, Chile, Namibia, and Australia are frequently chosen for networks. These regions are positioned around the globe at somewhat regular intervals and so selecting stations from them provides nearly continuous probe coverage. Also, for areas in Chile and Namibia, CFLOS values are very high, ≥ 74 %, further increasing the network availabilities. Stations in Europe and South Africa are rarely selected in optimal networks.

It is desirable for stations in a practical optical network to be located at higher altitudes to reduce beam scatter and modulation due to aerosols and turbulence. With minimum station altitudes of ≥ 1.5 km, selected network stations are primarily in the northern hemisphere whether the probe is in northern or southern declination. Most of the land mass for these altitudes are located in the northern hemisphere. As a result, stations in Israel, Uzbekistan, Hawaii, and China become more common in optimal networks. Stations in Chile are always present in the these networks as a result of high altitudes and high CFLOS.

The declination of a Mars probe in this study cycles between northern and southern latitudes over the course of an approximately 18 month cycle. When the probe is in a more northern declination, coverage is higher for northern hemisphere regions than for southern hemisphere regions, resulting in more northern hemisphere stations in the optimal networks. When the probe is in a more southern declination, more southern hemisphere stations occur in the networks. However, stations in southwestern CONUS and Chile are almost always present in a network no matter where the probe is. The networks presented here will likely be different for different probe orbits such as for the Moon and Saturn.

The networks in this study were generated with one year of data (June 2003 – May 2004). To ensure fidelity

of network statistics, more years of data are needed to account for cyclic changes in atmospheric circulations, such as El Niño/La Niña patterns. The data that is needed includes satellite data as well as surface observations. In many of the worldwide regions examined in this study, in particular Namibia and China, surface observations are sparse. The lack of data leads to missing masks for many time periods. To reduce the number of missing time steps and to increase the accuracy of the cloud masks, other sources of surface data must be identified and the CMG must be changed to include such data. Perhaps these extra data sources will help to solve CMG's considerable underprediction of low clouds at night in certain humid environments such as southwest Australia and the Canary Islands.

This study demonstrates that a ground station network for deep space to ground laser communications with an availability of 90 % or greater is feasible with a minimum of five stations based only on cloud cover and probe position. Our calculations do not consider the effect of optical turbulence or atmospheric aerosol loading which can also disrupt laser communications. Equipment trouble at ground stations will also further reduce network availability. All of these factors must be considered in the ultimate selection of ground stations for a lasercom network.

5. REFERENCES

Allen, A. C., Jr., P. A. Durkee, and C. H. Wash, 1990: Snow/cloud discrimination with multispectral satellite measurements. *Journal of Applied Meteorology*, **29**, 994–1004.

Alliss, R. J., R. L. Link, and M. E. Craddock, 2004: Mitigating the impact of clouds on optical communications. *13th Conference on Satellite Meteorology and Oceanography*, Norfolk, VA.

Alliss, R. J., M. E. Loftus, D. Apling, and J. Lefever, 2000: The development of cloud retrieval algorithms applied to GOES digital data. *10th Conference on Satellite Meteorology and Oceanography*, American Meteorological Society, Long Beach, CA, 330–333.

Ellrod, G. P., 1995: Advances in the detection and analysis of fog at night using GOES multispectral infrared imagery. *Weather and Forecasting*, **10**, 606–619.

Hunt, G. E., 1973: Radiative properties of terrestrial clouds at visible and infrared thermal window wavelengths. *Quarterly Journal of the Royal Meteorological Society*, **99**, 346–359.

Lee, T. F., F. J. Turk, and K. Richardson, 1997: Stratus and fog products using GOES-8 3.9 μm data. *Weather and Forecasting*, **12**, 664–677.

Link, R. L., M. E. Craddock, and R. J. Alliss, 2005: Mitigating the impact of clouds on optical communications. *2005 IEEE Aerospace Conference*, IEEE, Big Sky, MT.

Piazzolla, S., F. Amoozegar, and R. Cesarone, 2004: Analysis of telescope site selection for optical deep space network. *2004 IEEE Aerospace Conference*, IEEE, Big Sky, MT, 1687–1695.

Press, W. H., S. A. Teukolsky, W. T. Vetterling, and B. P. Flannery, 1994: *Numerical Recipes in C 2nd Edition*. Cambridge University Press, 994 pp.

Setvák, M. and C. A. Doswell, III, 1991: The AVHRR channel 3 cloud top reflectivity of convective storms. *Monthly Weather Review*, **119**, 841–847.

Shaik, K., D. Wonica, and M. Wilhelm, 1993: Optical subnet concepts for the deep space network. Technical report, NASA/Jet Propulsion Laboratory, telecommunications and Data Acquisition Progress Report 42-115.

Wojcik, G. S., H. L. Szymczak, R. J. Alliss, R. P. Link, M. E. Craddock, and M. L. Mason, 2005: Deep-space to ground laser communications in a cloudy world. *Proceedings of SPIE Free-Space Laser Communications V*, SPIE, San Diego, CA, 589203–1 – 589203–11.

6. ACKNOWLEDGMENTS